Kinetics of the Reaction of Nitric Oxide with Hydrogen

W. L. Flower, R. K. Hanson and C. H. Kruger
Department of Mechanical Engineering
Stanford University, Stanford, Calif.

SUMMARY

The reaction of nitric oxide with hydrogen has been studied in the temperature range 2400–4500°K using a shock-tube technique. Mixtures of NO and H_2 diluted in argon or krypton were heated by incident shock waves, and the infrared emission from the fundamental vibration-rotation band of NO at 5.3 microns was used to monitor the time-varying NO concentration. The decomposition of nitric oxide behind the shock was found to be modeled well by a fifteen-reaction system. A principle result of the study was the determination of the rate constant for the reaction $H + NO \overset{1}{\rightarrow} N + OH$, which may be the rate-limiting step for NO removal in some combustion systems. Experimental values of k_1 were obtained for each test through comparisons of measured and numerically predicted NO profiles. The data are fit closely by the expression $k_1 = 1.34 \times 10^{14} \exp(-49,200/RT)$ cm^3/mole-sec. These data appear to be the first available for this rate constant.
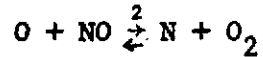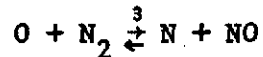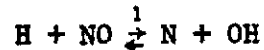
I INTRODUCTION

The kinetics of nitric oxide removal are of current interest in studies of combustion kinetics and air pollution. A principal mechanism for removing NO is provided by the reactions

$$O + NO \overset{2}{\rightleftharpoons} N + O_2$$

and

$$O + N_2 \overset{3}{\rightleftharpoons} N + NO$$

generally called the Zel'dovich mechanism. The additional reaction

$$H + NO \overset{1}{\rightleftharpoons} N + OH$$

may be of importance in combustion systems, particularly during fuel-rich operation. Reactions (1)-(3) are sometimes referred to as the extended Zel'dovich mechanism. The forward rate constants for reactions (1) and (2) are of particular interest as reactions (1) and (2) are often rate-limiting steps in NO removal, the reverse of reaction (3) being exothermic and proceeding rapidly once N atoms are formed.

Measurements of k_2 in the temperature range 2500-4100°K have been made recently in this laboratory by Hanson, et al.[1] The intent of the current study was to complement this previous work by investigating the reaction of atomic hydrogen with nitric oxide so that reliable rate constant data for both rate-controlling reactions (1 and 2) would be available for use in the kinetic modeling of nitric oxide decomposition. The measurement of k_1 is of particular importance as no experimental data are available, and previous estimates of this rate constant are based only on low-temperature measurements of the rate constant for the reverse reaction.[2,3]

The technique used in the present study involved shock-heating mixtures of NO, H_2, and an inert gas, either argon or krypton, and monitoring the decay of infrared emission from the fundamental vibration-rotation band of NO at 5.3 microns. For initial NO:H_2 ratios between 2:1 and 1:2, reaction (1) was found to dominate the removal of NO at early times. Hence the

rate constant for reaction (1) could be determined accurately by choosing k_1 to provide the best agreement between experimental NO concentration records and numerical solutions to the coupled gasdynamic and chemical kinetic equations.

II EXPERIMENTAL

The experiments were carried out in a stainless steel shock tube with an inner diameter of 15 cm. The plastic diaphragms (lexan, 0.5 to 1.2 mm thick) used in the tests were ruptured by increasing the driver pressure until the plastic was punctured by a crossed-knife arrangement fixed downstream. The reproducibility of shock strength was excellent using this method. The driver gas was helium; a maximum driver pressure of 13 atmospheres was required.

Incident shock speeds, which varied from 1.43 to 1.99 mm/μsec, were measured by means of four platinum thin-film resistance thermometers mounted flush with the inside surface of the tube. The signals from these gauges were used to trigger three time-interval counters. The uncertainty in shock speed at the observation station was less than ± 0.2% which leads to an uncertainty in reaction temperature of less than 0.4%. The influence of shock speed attenuation and concomitant boundary layer effects on temperature was somewhat larger, but still may be neglected here because the rate constant k_1 is determined from data obtained relatively near the shock front. Attenuation in shock speed varied up to 1% per meter. The initial temperature T_1 varied from 292° to 297°K.

The shock tube was evacuated with a large diffusion pump to a pressure of 10^{-5} torr or lower. The residual leak and outgassing rate was about 10^{-5} torr per minute. Mixtures of NO, H_2 and an inert gas, either argon or krypton, were prepared immediately before each run in a stainless steel mixing tank (total pressures up to 25 psia) with an externally driven stirring rod. The

initial pressure of the test gas mixture varied from 4.4 to 17.3 torr and was determined from the measured pressure in the mixing tank and its known volume relative to that of the shock tube.

The NO, H_2, Ar and Kr used in these experiments were obtained from commercial cylinders without further purification. The NO was purchased from Liquid Carbonic (typical purity claimed to be 99.0%) and later analyzed for NO_x and N_2 content using an NO_x chemiluminescent detector and standard gas chromatography. Significant impurities in the NO were 0.82% N_2 and 0.66% N_2O; a negligible amount of NO_2 was found. The H_2 was research grade with a minimum purity of 99.999% claimed by Liquid Carbonic. Compositions corrected for the measured impurities in the NO were used in the data reduction.

The initial H_2 concentrations ranged from 10% of the initial NO concentration to double the amount of NO used. Nominal $NO:H_2$ ratios for most experiments were either 2:1, 1:1, or 1:2, and the inert gas (either argon or krypton) made up no less than 85% (by volume) of the test gas for any test.

Observations of the infrared emission from the fundamental vibration-rotation band of NO at 5.3 microns were made behind incident shock waves using the arrangement shown schematically in Fig. 1. The InSb detector (liquid nitrogen cooled, 1 mm x 3 mm active element) was imaged on the inner surface of the nearest window using a large (12.5 cm diam, 30 cm focal length) off-axis parabolic mirror set at approximately unity magnification. Alignment and focusing were accomplished using a simple tensor lamp and lens located on the opposite side of the tube. The flat sapphire windows (8 mm diam, 2 mm thick) were mounted nearly tangent to the inner contour of the tube so that the maximum perturbation to the flow was 0.2 mm.

The spatial resolution of the system was varied with an adjustable slit placed 38 cm from the tube. The slit widths employed varied from 1.5 to 4 mm and were selected on the basis of signal strength and spatial resolution requirements.

The detector was coupled to a wide-bandwidth transimpedance amplifier

(13 kΩ transimpedance, 2 MHz bandwidth) whose output was displayed directly on an oscilloscope (Telequipment D-83). The time base and vertical amplifier of the oscilloscope were carefully adjusted and calibrated to optimize the accuracy of the data. The overall circuit response time to a step in radiation was measured (with the adjustable slit nearly shut) to be about 1 μsec, which was quite adequate for the present work.

In the present experiments the NO is optically thin, or very nearly thin, so the infrared radiation from the fundamental ($\Delta v = 1$) vibration-rotation band is directly proportional to the energy stored in vibration. Following the infrared emission behind the shock wave is therefore equivalent to monitoring the product of the molar concentration and the average vibrational energy per mole. Thus if V is the output voltage of our linear detector, and I represents the intensity of spontaneous emission in the line of sight of the detector,

$$V = C_1 I = C_2 [NO] L e_v (T) \tag{1}$$

where [NO] is the concentration of NO, L is the tube diameter, C_1 and C_2 are unspecified proportionality constants and $e_v(T)$ is the vibrational energy of NO at temperature T,

$$e_v = R \theta / [\exp (\theta/T) - 1].$$

A harmonic oscillator model is assumed where θ is the characteristic vibrational temperature (2740°K for NO) and R is the universal gas constant. Vibrational equilibration at the local translational temperature is also assumed as NO has a very short relaxation time[4]. To eliminate the need for absolute calibration as well as for convenience in comparing measured and calculated NO histories, the signal magnitude may be normalized by its initial value behind the shock so that

$$V(t)/V_o = \frac{[NO]}{[NO]_o} \frac{e_v(T)}{e_v(T_o)} \tag{2}$$

The proportionality between signal magnitude and the product of the nitric oxide concentration and the NO vibrational energy, Eq. (1), holds
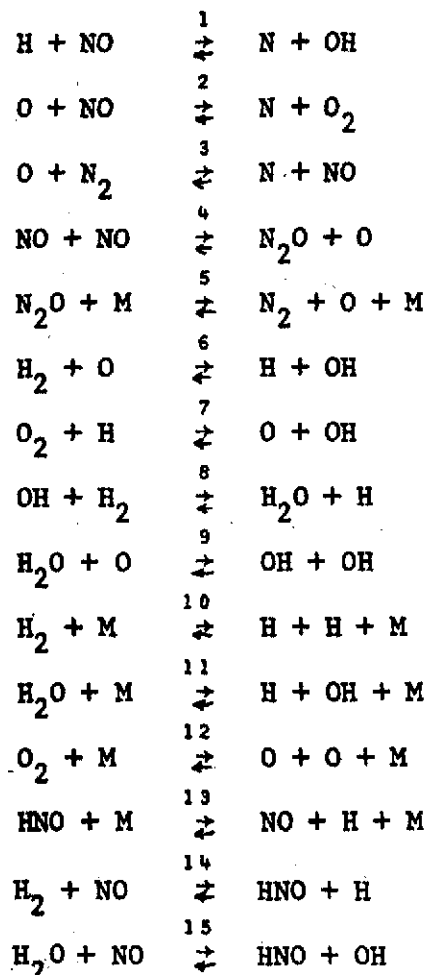
strictly only if radiation from the entire NO fundamental is measured and a detection system with a uniform spectral response is employed. In the present experiments, only the radiation in the spectral region of approximately 5.0-5.4 microns was measured since a filter passing radiation of wavelength greater than 5.0 microns was used and the response of the InSb detector falls off sharply for wavelengths longer than 5.4 microns. The band center of the NO fundamental vibration-rotation band coincides very nearly with the long-wavelength cutoff of the infrared detection system, and the bandhead of the R branch of the NO fundamental is located at 4.94 microns, close to the short-wavelength cutoff of the detection system. Hence, most of the R branch radiation and relatively little radiation from the P and Q branches is measured by the infrared detection system. In the simplest approximation then, Eqs. (1) and (2) are still expected to apply with only a change in the proportionality constants in Eq. (1) to account for the filter and detector used; our experimental data justify this approximation for the conditions of the present experiments. Actually, the particular temperature dependence employed for the relation of NO concentration to detector signal is not critical, since temperature was nearly constant for each experiment. Typically $e_v(T)/e_v(T_0)$ varied by only a few per cent for the portion of the NO decomposition studied here; in the two extreme cases, the factor reached a minimum value of 0.92 and a maximum of 1.04.

A typical data trace for an experiment at 3600°K is shown in Fig. 2. The signal is seen to rise to a peak at the shock front and thereafter to decay monotonically toward equilibrium. Records obtained with slower sweep speeds confirm that the signals approach the expected, near-zero equilibrium values for the higher temperature experiments. For the experiments at lower temperatures and smaller $[NO]/[H_2]$ ratios, the signal approached a small (relative to the initial signal immediately after the shock) but obviously non-zero magnitude. Several shocks in H_2-O_2-Argon mixtures indicated that this small

final signal level was due to radiation from the 6.3-micron band of H_2O. To minimize the effect of the H_2O radiation on the determination of k_1, only the first portion of the signal record ($[NO]/[NO]_o > .6$ to $.7$) was analyzed in the data reduction for the lower temperature ($T \lesssim 3000°K$) experiments.

III   DATA REDUCTION AND RESULTS

The kinetics of the decomposition of nitric oxide were modeled using the following fifteen-reaction system:

$$H + NO \overset{1}{\rightleftarrows} N + OH$$

$$O + NO \overset{2}{\rightleftarrows} N + O_2$$

$$O + N_2 \overset{3}{\rightleftarrows} N + NO$$

$$NO + NO \overset{4}{\rightleftarrows} N_2O + O$$

$$N_2O + M \overset{5}{\rightleftarrows} N_2 + O + M$$

$$H_2 + O \overset{6}{\rightleftarrows} H + OH$$

$$O_2 + H \overset{7}{\rightleftarrows} O + OH$$

$$OH + H_2 \overset{8}{\rightleftarrows} H_2O + H$$

$$H_2O + O \overset{9}{\rightleftarrows} OH + OH$$

$$H_2 + M \overset{10}{\rightleftarrows} H + H + M$$

$$H_2O + M \overset{11}{\rightleftarrows} H + OH + M$$

$$O_2 + M \overset{12}{\rightleftarrows} O + O + M$$

$$HNO + M \overset{13}{\rightleftarrows} NO + H + M$$

$$H_2 + NO \overset{14}{\rightleftarrows} HNO + H$$

$$H_2O + NO \overset{15}{\rightleftarrows} HNO + OH$$

Note that all reactions are written in the endothermic direction. Selection of the above reaction mechanism was based in part on the authors' previous study of nitric oxide decomposition [1]   and on the many studies of the H_2-O_2 reaction (for example, Asaba, et al.)[5].   A number of other reactions, notably several involving NO_2 or HO_2, were included in the reaction mechanism for trial numerical solutions of the kinetic equations. These reactions were found to have virtually no influence on the predictions of NO concentrations. The three reactions involving HNO, (13)-(15), had only a slight influence on calculated NO histories and could be totally deleted from the reaction system with little loss of accuracy (for the purposes of the present study).

Numerical solutions to the kinetic and gasdynamic equations were obtained

using the NASA Lewis general chemical kinetics computer program[6]. For-ward rate constants for reactions (2)-(15) were evaluated using the expressions listed in Table I. The reverse of each reaction was also incorporated in the computations, with the reverse rate constants determined from the forward rates using equilibrium constants based on the JANAF Thermochemical Tables.[13]

Since no previous determination of the rate constant for reaction (1) was available, the value used in our initial kinetic calculations had to be estimated from low temperature measurements of the reverse rate constant, k_{-1}. Campbell and Thrush[2] determined that $k_{-1}/k_{-7} = 1.4 \pm 0.1$ at 300°K. Combining this with the value for k_{-7} obtained by Clyne and Thrush[14], we obtain the value $k_{-1} = 4.1 \times 10^{13}$ cm^3/mole-sec at 300°K. No estimate of the temperature dependence of k_{-1} was made by Campbell and Thrush, but the temperature dependence has generally been assumed to be small. Several authors have used the same numerical value of $k_{-1} = 4.1 \times 10^{13}$ cm^3/mole-sec at temperatures up to 3000°K[15,16].

For our first calculations, we chose to assume $k_{-1} = 4.1 \times 10^{13}$ cm^3/mole-sec, independent of temperature, and calculated k_1 using the equilibrium constant. Revised estimates of k_1 were obtained by comparing calculated histories of $[NO]e_v(T)/([NO]_o e_v(T_o))$ to the experimental records of the normalized detector signal, V/V_o, and choosing k_{-1} (and hence k_1) for each test so as to produce the best agreement between the numerical predictions and the data.

Pertinent data regarding each of 22 experiments in the temperature range 2400-4500°K are summarized in Table II. $T_{2,frozen}$ is the temperature immediately behind the shock front calculated assuming vibrational equilibrium and frozen composition. $T_{2,average}$ and P_2 in Table II are average values for the portion of the NO decomposition which was studied in obtaining the fit between calculated and measured NO time histories. Typically, the fit was made for that region of the curve in which [NO] decreased to 30-40% of its initial value. $k_1(T_{2,ave})$ is the value of the forward rate constant for reaction (1) obtained from combining

the reaction equilibrium constant (evaluated at $T_{2,ave}$) with the constant value of k_{-1} which best fit the data.

Two important points should be noted regarding the approach used to determine the value of k_1 for each experiment. First, since the reverse rate constant is chosen to be the temperature-independent value which provides the best agreement between the numerical calculations and experiment, we in effect have assumed that the forward rate constant has an activation energy equal to the endothermicity of reaction (1) for each experiment. However, in any particular experiment the temperature did not vary greatly. Hence the specified temperature dependence does not significantly effect the value of $k_1(T_{2,ave})$ determined for each experiment.

Secondly, the value of k_1 inferred with the other rate constants held fixed can be accurate only if the predicted [NO] profiles are more sensitive to small changes in k_1 than to reasonable variations in the other rate constants. Careful studies of individual rate constant sensitivity were performed for several representative experiments to verify the dominance of k_1. The sensitivity analysis for one particular experiment will be discussed in greater detail. However, the calculations in all cases confirmed that predicted NO concentrations were most sensitive to changes in k_1. Individual variations of other rate constants within the estimated uncertainties of each (most were obtained from Baulch, et al.[10, 12])in no case produced changes in the predicted NO profiles (for $[NO]/[NO]_o > .4$) greater than produced by a 20-30% change in k_1.

The fit of the kinetic calculations to the data and the sensitivity of the calculations to the value chosen for k_1 are shown in Fig. 3 for run 13 ($T_{2,ave}$ = 3605°K). The middle curve represents the NO record predicted using the value of k_1 which gave the best fit to the data. Shown for comparison are the numerical solutions obtained when the values of k_1 used in the calculations were larger and smaller than the selected value by a factor of 1.4.

Note that the abscissa in Fig. 3 is laboratory time, t_{lab}, related to the distance x behind the shock front by $t_{lab} = x/V_s$. The shock speed, V_s, was assumed constant in the numerical integration of the governing equations. The

factor used to approximate the temperature dependence of the relation between

NO concentration and detector signal is $f(T) = e_v(T) = R\theta/[\exp(\theta/T)-1]$.

The primary uncertainty in plotting the data points for V/V_o in Fig. 3 is

the uncertainty in determining V_o from the oscilloscope record. The maximum

voltage observed on the oscilloscope trace was used for normalization of the

voltages. The actual voltage which would correspond to the initial NO concentra-

tion behind the shock is not visible because of imperfect resolution of the

shock front discontinuity when a finite element of gas is viewed by the detector.

We estimate that the proper V_o to characterize the actual $[NO]_o$ might be as much

as 2% to 3% greater than the value of V_o used to normalize the data in Fig. 3.

Such an increase in V_o would lead to a slight downward displacement in the location

of the data points in Fig. 3 and a negligible change in the value of k_1 selected.

The relative insensitivity of the calculated NO concentrations for the same

experiment to large variations in the rate constants for the reactions

$$O + NO \overset{2}{\rightleftarrows} N + O_2$$

and $$NO + NO \overset{4}{\rightleftarrows} N_2O + O$$
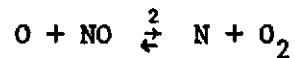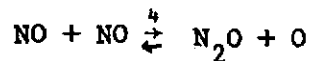
is shown in Fig. 4. For comparison the curves for k_1 factors of $(1.4)^{\pm 1}$ different

from the selected value have been plotted again.

The factor of 5 by which the rate constant for reaction (2) has been

increased here is far greater than the 20% reasonable uncertainty in this rate

constant[1] but still has only a slight effect compared to a 40% increase in k_1.

For other experiments, particularly those with higher initial $[NO]/[H_2]$ ratios,

the sensitivity of the calculations to changes in k_2 is greater. However, even

for the two shocks for which $[NO]_o/[H_2]_o \approx 10$, 20% variations in k_1 clearly

produce a greater effect on the numerical NO predictions than do 20% changes

in the value of k_2 used in the calculations.

Figure 5 shows the sensitivity of the kinetic calculations to variations

in the rate constants for three reactions of the H_2-O_2 system:

$$H_2 + O \overset{6}{\rightleftarrows} H + OH$$

$$OH + H_2 \overset{8}{\rightleftarrows} H_2O + H$$

$$H_2 + M \overset{10}{\rightleftarrows} H + H + M$$
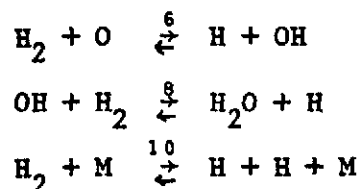
The results for variations in k_6 and k_8 typify the insensitivity of the kinetic calculations to changes in the rate constants for the fast exchange reactions involving OH, reactions (6) - (9). Baulch, et al.[10] recommend uncertainties of only 30-50% for these four reactions (but for temperatures up to 2000-2500°K, so the uncertainty at the highest temperatures under study here would be somewhat greater). The effect shown by a factor of 2 increase in the rate constant for reaction (10) is of greater significance, since Baulch, et al.[10] recommend a factor of 2 uncertainty in this rate for the full temperature range under study here. Clearly the accuracy with which k_1 may be determined by this method is limited by the uncertainty in k_{10}.

Values of k_1 representing the best fit to the data of each experiment are plotted in Fig. 6. Each data point corresponds to the magnitude of k_1 evaluated at $T_{2,ave}$. The error bar on the data point for run 13 represents an uncertainty of ± 30%, which we estimate to be the maximum reasonable uncertainty in the determination of k_1 for that run due to uncertainties in the data, selecting the best fit to the data and the possible errors in the other rate constants. The line which best fits all of the experimental values of k_1, when plotted in Arrhenius form, has been calculated by the method of least squares. The best fit gives the rate expression

$$k_1 = 1.34 \times 10^{14 \pm \cdot 06} exp \{-(49,200 \pm 800)/RT\} \ cm^3/mole\text{-}sec \qquad (3)$$

which has been plotted in Fig. 6. The standard deviations of the estimates of the pre-exponential factor and the activation energy are indicated in Eq. (3).

There appears to be no other direct measurement of k_1 with which to compare these results. The activation energy we have determined is reasonable, being slightly greater than the 47,300 cal/mole heat of reaction at 3500°K. Equation (3) thus predicts a small activation energy of 1900±800 cal/mole for the reverse reaction at this temperature. Extrapolating Eq. (3) to lower temperatures

and dividing by the equilibrium constant K_1, we obtain $k_{-1} = 1.3 \times 10^{13} cm^3$/mole-sec at 300°K. Although this result is approximately one third of the value for k_{-1} at 300°K recommended by Campbell and Thrush[2], the disagreement is not significant in view of the lengthy extrapolation and the uncertainty in the activation energy. Our result is also consistent with Garvin and Broida's determination that $k_{-1} > 6 \times 10^{12} cm^3$/mole-sec at ambient temperatures[3].

Since k_1 is 2-3 times the rate constant for $O + NO \xrightarrow{2} N + O_2$ at combustion temperatures, we conclude that reaction (1) may indeed be important in modeling NO decomposition in combustion systems, particularly for fuel-rich conditions.

ACKNOWLEDGMENTS

REFERENCES

1   Hanson, R. K., Flower, W. L., and Kruger, C. H.: Combustion Sci. Tech., in press.

2   Campbell, I. M. and Thrush, B. A.: Trans Faraday Soc. 64, 1265 (1968).

3   Garvin, D. and Broida, H. P.: Ninth Symposium (International) on Combustion, p. 678, Academic Press, 1963.

4   Wray, K. L.: J. Chem. Phys. 36, 2597 (1962).

5   Asaba, T., Gardiner, Jr., W. C. and Stubbeman, R. F.: Tenth Symposium (International) on Combustion, p. 295, The Combustion Institute, 1965.

6   Bittker, D. A. and Scullin, V. J.: General Chemical Kinetics Computer Program for Static and Flow Reactions, with Application to Combustion and Shock-Tube Kinetics, NASA TN D-6586, 1972.

7   Wray, K. L. and Teare, J. D.: J. Chem. Phys. 36, 2582 (1962).

8   Jost, V. W., Michel, K. W., Troe, J., and Wagner, H.: Z. Naturforschung 19A, 59 (1964).

9   Flower, W. L., Hanson, R. K., and Kruger, C. H.: Investigation of Nitric Oxide Decomposition in the Temperature Range 2500-4100°K. Paper presented at the 1974 Spring Meeting of the Western States Section of the Combustion Institute, Pullman, Wash.

10   Baulch, D. L., Drysdale, D. D., Horne, D. G., and Lloyd, A. C.: Evaluated Kinetic Data for High Temperature Reactions, Vol 1, CRC Press, 1972.

11   Camac, M. and Vaughan, A.: J. Chem Phys. 34, 460 (1961).

12   Baulch, D. L., Drysdale, D. D., Horne, D. G., and Lloyd, A. C.: Evaluated Kinetic Data for High Temperature Reactions, Vol 2, CRC Press, 1973

13   JANAF Thermochemical Tables, Second Edition, National Bureau of Standards (1971).

14   Clyne, M. A. A. and Thrush, B. A.: Proc. Roy. Soc. A. 275, 544 (1963).

15   Lavoie, G. A., Heywood, J. B., and Keck, J. C.: Combustion Sci. Tech. 1, 313 (1970).

16   Bowman, D. T.: Combustion Sci. Tech. 3, 37 (1971).

Table I

Rate Constant Expressions

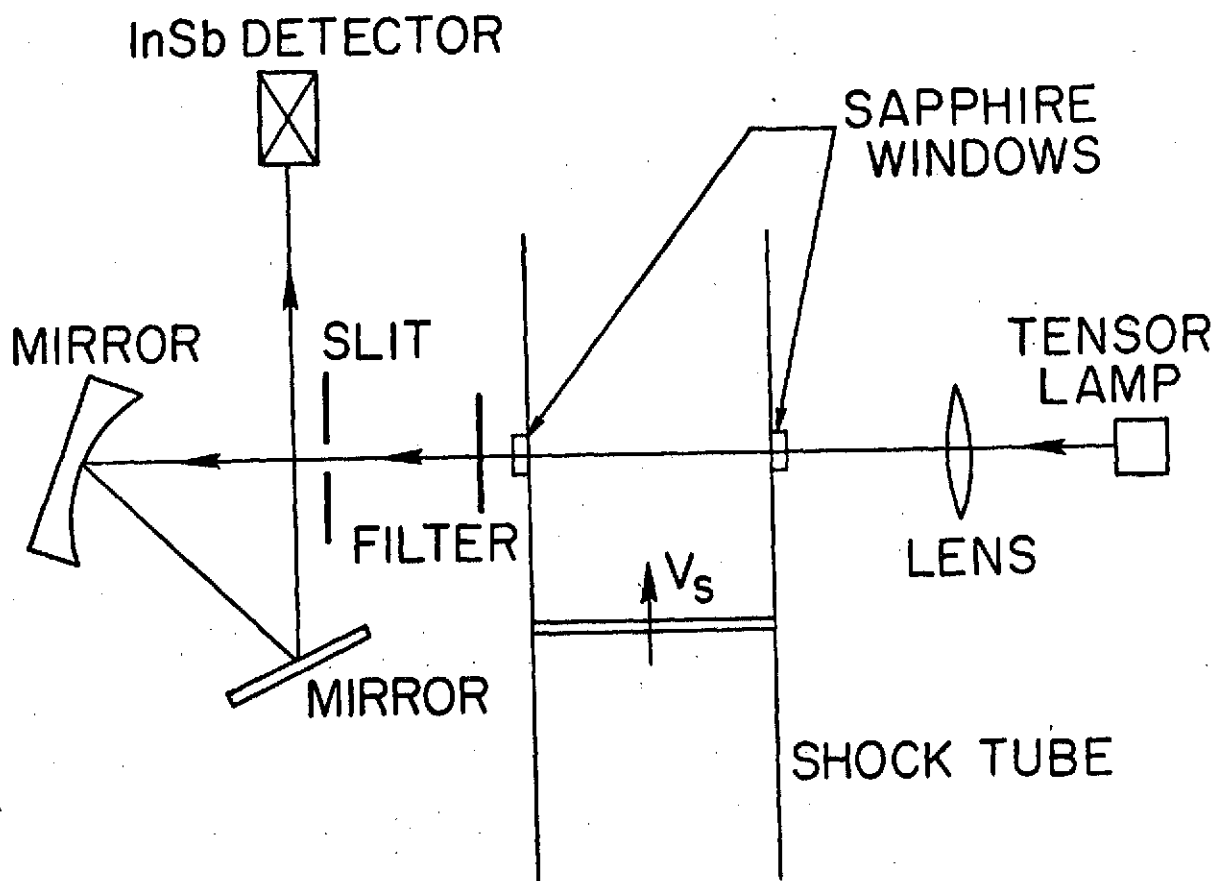| Reaction	Rate Constant, in direction indicated $\dagger$ cm^3/mole-sec	References
NO + O $\overset{2}{\rightarrow}$ N + O_2	2.36×10^9 T $\exp(-38{,}640/RT)$	Hanson, et al. (1974)[1]
O + N_2 $\overset{3}{\rightarrow}$ N + NO	7.0×10^{13} $\exp(-75{,}500/RT)$	Wray and Teare (1962)[7]
NO + NO $\overset{4}{\rightarrow}$ N_2O + O	5.7×10^{12} $\exp(-63{,}800/RT)$	Our estimate, $k_4 \equiv -(1/2)[NO]^{-2}d[NO]/dt$
N_2O + M $\overset{5}{\rightarrow}$ N_2 + O + M	1.0×10^{15} $\exp(-61{,}000/RT)$	Jost, et al. (1964)[8] Flower, et al. (1974)[9]
H_2 + O $\overset{6}{\rightarrow}$ H + OH	1.8×10^{10} T $\exp(-8900/RT)$	Baulch, et al. (1972)[10]
O_2 + H $\overset{7}{\rightarrow}$ O + OH	2.2×10^{14} $\exp(-16{,}800/RT)$	Baulch, et al. (1972)[10]
OH + H_2 $\overset{8}{\rightarrow}$ H_2O + H	2.2×10^{13} $\exp(-5150/RT)$	Baulch, et al. (1972)[10]
H_2O + O $\overset{9}{\rightarrow}$ OH + OH	6.8×10^{13} $\exp(-18{,}360/RT)$	Baulch, et al. (1972)[10]
H_2 + M $\overset{10}{\rightarrow}$ H + H + M	8.8×10^{14} $\exp(-96{,}000/RT)$, M = H, H_2 2.2×10^{14} $\exp(-96{,}000/RT)$, M = other species	Baulch, et al. (1972)[10]
H_2O + M $\overset{11}{\rightarrow}$ H + OH + M	2.2×10^{16} $\exp(-105{,}100/RT)$, M = H_2O 1.3×10^{15} $\exp(-105{,}100/RT)$, M = other species	Baulch, et al. (1972)[10]
O_2 + M $\overset{12}{\rightarrow}$ O + O + M	3.55×10^{18} $T^{-1}\exp(-118{,}000/RT)$	Camac and Vaughan (1961)[11]
NO + H + M $\overset{-13}{\rightarrow}$ HNO + M	5.4×10^{15} $\exp(+596/RT)$	Baulch, et al. (1973)[12]
HNO + H $\overset{-14}{\rightarrow}$ H_2 + NO	3.0×10^{11} $T^{1/2}\exp(-2385/RT)$	Baulch, et al. (1973)[12]
HNO + OH $\overset{-15}{\rightarrow}$ H_2O + NO	3.0×10^{12} $T^{1/2}\exp(-2385/RT)$	Baulch, et al. (1973)[12]

$\dagger$ Note that the reverse rate constant is specified for reactions (13),(14),(15) as no data are available for the forward rates.

Table II

Experimental Conditions and Data

	Composition (balance: Ar for #1-11, Kr for #12-22)		P_1 (torr)	V_s (mm/μsec)	T_2 (°K)		P_2 (atm)	$k_1(T_{2,ave})$ (cm³/mole-sec)
	% NO	% H_2			frozen	average		
1	4.0	8.1	17.3	1.640	2348	2365	.70	4.40×10^9
2	4.0	8.1	15.7	1.652	2381	2395	.64	4.54×10^9
3	4.0	4.1	15.7	1.625	2434	2440	.64	5.19×10^9
4	5.0	10.2	11.3	1.772	2601	2600	.53	9.00×10^9
5	5.0	5.1	13.8	1.708	2605	2625	.62	9.82×10^9
6	4.9	5.0	11.5	1.730	2670	2670	.53	1.15×10^{10}
7	4.9	5.0	5.0	1.819	2923	2960	.25	3.52×10^{10}
8	4.9	5.0	5.1	1.877	3091	3100	.28	4.41×10^{10}
9	9.9	1.0	5.1	1.859	3085	3105	.28	5.36×10^{10}
10	4.9	5.0	5.0	1.911	3195	3195	.28	6.10×10^{10}
11	4.9	5.4	4.4	1.991	3427	3420	.26	9.52×10^{10}
12	6.6	3.4	6.1	1.428	3625	3600	.40	1.35×10^{11}
'3	5.0	5.1	6.1	1.435	3640	3605	.40	1.21×10^{11}
14	3.3	6.7	6.1	1.468	3780	3720	.41	1.35×10^{11}
	4.7	5.0	6.7	1.499	3956	3860	.48	2.41×10^{11}
16	5.8	6.0	6.9	1.566	4177	4080	.53	2.81×10^{11}
17	7.3	7.5	4.5	1.620	4271	4120	.37	2.53×10^{11}
18	8.8	1.0	6.7	1.532	4163	4150	.51	4.03×10^{11}
19	5.9	3.1	6.9	1.565	4347	4265	.54	4.35×10^{11}
20	6.9	3.6	5.9	1.606	4475	4390	.48	5.10×10^{11}
21	5.3	5.3	6.0	1.629	4571	4420	.51	5.30×10^{11}
22	6.4	3.5	6.2	1.614	4552	4450	.52	5.95×10^{11}

FIGURE CAPTIONS

Figure 1:   Infrared optical system.

Figure 2:   Oscilloscope data trace for run 13 showing voltage record from infrared detector as a function of laboratory time. Vertical sensitivity = 4 mV/div., sweep speed = 20 μsec/div.

Figure 3:   Comparison of measured values of V/V_0 (O) for run 13 with calculated values of $[NO]\, f(T)/\{[NO]_0\, f(T_0)\}$. The temperature dependent factor $f(T)$ has been approximated by $e_v(T) = R\Theta/[\exp(\Theta/T)-1]$ (see text). Best-fit calculations used $k_{-1} = 3.81 \times 10^{13} cm^3/mole\text{-}sec$ with k_1 obtained using the equilibrium constant. Shown for comparison are calculations made using $k_1 = 1.4 \times (k_1)_{best\ fit}$ and $k_1 = (k_1)_{best\ fit}/1.4$.

Figure 4:   Sensitivity of calculated normalized NO concentrations to individual rate constants for run 13. Calculations shown by solid lines used $k_1 = 1.4 \times (k_1)_{best\ fit}$, and $k_1 = (k_1)_{best\ fit}/1.4$ together with the rate constants in Table I. Other calculations used $(k_1)_{best\ fit}$ and the rate constants in Table I (indicated by primes) except as noted: —— · —— , $k_2 = 5 \times k_2'$; — — — — — — , $k_4 = 2 \times k_4'$.

Figure 5:   Sensitivity of calculated normalized NO concentrations to individual rate constants for run 13. Calculations used $k_{-1} = 3.81 \times 10^{13} cm^3/mole\text{-}sec$ and the rate constants in Table I (indicated by primes) except as noted: —— · —— , $k_6 = k_6'/10$, —— — —— $k_8 = 5 \times k_8'$, — — — — — — , $k_{10} = 2 \times k_{10}'$.

Figure 6:   Arrhenius plot for the reaction $H + NO \overset{1}{\rightarrow} N + OH$. The solid line represents a least squares fit to the data of the present study (O) and is defined by the equation $k_1 = 1.34 \times 10^{14} \pm {}^{.06} \exp\{-(49{,}200 \pm 800)/RT\}$ $cm^3/mole\text{-}sec$. The error bar indicates the estimated ±30% maximum reasonable uncertainty in the determination of k_1 for run 13.

NO IR Emission Record

Figure: Plot of $[NO]\,f(T)/\{[NO]_0\,f(T_0)\}$ versus t_{LAB} (μsec). Curves labeled $k_6 = k_6'/10$, $k_{10} = 2k_{10}'$, and $k_8 = 5k_8'$.